Dynamic NMR Studies of Cationic Bis(2-phenylindenyl)zirconium Pyridyl Complexes: Evidence for *syn* Conformers in Solution

Alice L. Lincoln, Gregg M. Wilmes, and Robert M. Waymouth*

Department of Chemistry, Stanford University, Stanford, California 94305-5080

Received June 9, 2005

The conformationally dynamic unbridged metallocene (2-PhInd)$_2$ZrMe$_2$ (**1**) was activated with trispentafluorophenylborane (B(C$_6$F$_5$)$_3$, **B2**) or trityl tetrakispentafluorophenylborate ("trityl borate", [Ph$_3$C$^+$][B(C$_6$F$_5$)$_4^-$], **B4**) to generate the ion pair [(2-PhInd)$_2$ZrMe$^+$][MeB(C$_6$F$_5$)$_3^-$] (**2a**) or [(2-PhInd)$_2$ZrMe$^+$][B(C$_6$F$_5$)$_4^-$] (**2b**), respectively. Activation parameters for ion-pair separation were determined by line-shape analysis (**2a**: $\Delta H^{\ddagger}_{ips} = 20 \pm 1$ kcal/mol, $\Delta S^{\ddagger}_{ips} = 17 \pm 4$ eu; **2b**: $\Delta H^{\ddagger}_{ips} = 15 \pm 2$ kcal/mol, $\Delta S^{\ddagger}_{ips} = 13 \pm 7$ eu). For **2a**, a much slower B(C$_6$F$_5$)$_3$ dissociation−reassociation process was also observed ($\Delta G^{\ddagger}_{83°C} = 18.9 \pm 0.1$ kcal/mol). Both **2a** and **2b** were treated with a series of *o*-substituted pyridines, and the behavior of the resulting zirconocenium-pyridyl complexes (**3a**−**8b**) was studied by ^{1}H, ^{13}C, and ^{19}F NMR over the temperature range −100 to 100 °C. Below room temperature, ^{1}H NMR NOESY spectra revealed signals characteristic of a C_s-symmetric *syn* conformation.

Introduction

Conformationally dynamic group 4 bis(2-arylindenyl) are an intriguing class of olefin polymerization catalysts that generate polypropylenes with stereosequence distributions ranging from rigid isotactic to amorphous atactic to stereoblock elastomeric plastics depending on the experimental conditions.[1−3] For the neutral precatalyst (2-PhInd)$_2$ZrCl$_2$, X-ray crystallography and theoretical studies indicate that the C_2-symmetric *anti* and C_s-symmetric *syn* conformers represent low-energy conformations, with the *anti* conformer slightly more stable. The *anti* conformation becomes considerably more stable as the steric bulk on the aryl substituent increases.[1,4−6] We had proposed that the temperature and monomer concentration dependence of the stereospecificity of these catalysts is due to a competition between monomer insertion and conformational isomerization of the metallocene and proposed that the interconversion between enantiomeric *anti* conformers and at least one *syn* conformer was responsible for the generation of isotactic and atactic stereosequences (Scheme 1). Indirect support for this proposal was provided by the polymerization behavior of the MAO-activated silyl-bridged *rac* (*anti*) and *meso* (*syn*) analogues, which produce isotactic and atactic polypropylene, respectively.[7,8] Recently, Busico has proposed, on the basis of microstructural analysis of these polymers, that the achiral *syn* isomer can be disregarded as a source of the atactic stereosequences and that the generation of isotactic and atactic stereosequences is the results of the interconversion of chiral *anti* isomers at a rate competitive with propylene insertion. According to this proposal, short atactic stereosequences are generated by kinetic states where the rate of conformational isomerization is faster than propylene insertion.[9−11]

To provide more evidence for the accessible conformations, direct observation of the conformational states of the active species would be highly informative; however, this has proven extremely challenging. Activation of the dichloro or dialkyl metallocene precursors in the presence of olefin generates very small concentrations of the cationic catalyst that have thus far been observed by NMR only in a few specific cases.[12−17] Additionally, the lifetime of the polymer-bound complex is short, with the complex undergoing rapid chain transfer and β-hydride elimination. For this reason, much of our understanding of the conformational dynamics of 2-arylindenyl metallocenes stems from studies of the rotation rates of the neutral precatalysts in solution, which have been esti-

(1) Coates, G. W.; Waymouth, R. M. *Science* **1995**, *267*, 217−219.
(2) Lin, S.; Waymouth, R. M. *Acc. Chem. Res.* **2002**, *35*, 765−773.
(3) Resconi, L.; Cavallo, L.; Fait, A.; Piemontesi, F. *Chem. Rev.* **2000**, *100*, 1253−1345.
(4) Cavallo, L.; Guerra, G.; Corradini, P. *Gazz. Chim. Ital.* **1996**, *126*, 463−467.
(5) Pietsch, M. A.; Rappe, A. K. *J. Am. Chem. Soc.* **1996**, *118*, 10908−10909.
(6) Maiti, A.; Sierka, M.; Andzelm, J.; Golab, J.; Sauer, J. *J. Phys. Chem. A* **2000**, *104*, 10932−10938.
(7) Petoff, J. L. M.; Agoston, T.; Lal, T. K.; Waymouth, R. M. *J. Am. Chem. Soc.* **1998**, *120*, 11316−11322.
(8) Finze, M.; Reybuck, S. E.; Waymouth, R. M. *Macromolecules* **2003**, *36*, 9325−9334.
(9) Busico, V.; Castelli, V. V. A.; Aprea, P.; Cipullo, R.; Segre, A.; Talarico, G.; Vacatello, M. *J. Am. Chem. Soc.* **2003**, *125*, 5451−5460.
(10) Busico, V.; Cipullo, R.; Kretschmer, W. P.; Talarico, G.; Vacatello, M.; Van Axel Castelli, V. *Angew. Chem., Int. Ed.* **2002**, *41*, 505−508.
(11) Busico, V.; Cipullo, R.; Segre, A. L.; Talarico, G.; Vacatello, M.; Castelli, V. N. A. *Macromolecules* **2001**, *34*, 8412−8415.
(12) Sillars, D. R.; Landis, C. R. *J. Am. Chem. Soc.* **2003**, *125*, 9894−9895.
(13) Landis, C. R.; Rosaaen, K. A.; Uddin, J. *J. Am. Chem. Soc.* **2002**, *124*, 12062−12063.
(14) Landis, C. R.; Rosaaen, K. A.; Sillars, D. R. *J. Am. Chem. Soc.* **2003**, *125*, 1710−1711.
(15) Landis, C. R.; Sillars, D. R.; Batterton, J. M. *J. Am. Chem. Soc.* **2004**, *126*, 8890−8891.
(16) Liu, Z. X.; Somsook, E.; Landis, C. R. *J. Am. Chem. Soc.* **2001**, *123*, 2915−2916.
(17) Liu, Z. X.; Somsook, E.; White, C. B.; Rosaaen, K. A.; Landis, C. R. *J. Am. Chem. Soc.* **2001**, *123*, 11193−11207.

10.1021/om050473k CCC: $30.25
Publication on Web 10/18/2005

Scheme 1. Expected Low-Energy Conformations of [(2-PhInd)$_2$Zr(polymeryl)$^+$] Based on Calculated Low-Energy Conformations of the Neutral Catalyst Precursor (2-PhInd)$_2$ZrCl$_2$[a]

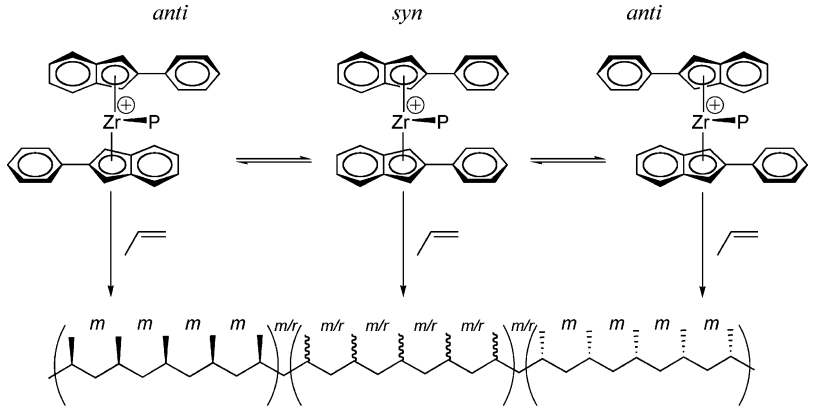

[a] For simplicity, the counteranion has not been depicted here.

mated previously from ^{1}H NMR data using line-shape analysis and on-resonance spin−lattice relaxation in the rotating frame ($T_1\rho$).[18−21] These studies reveal rapid rotation of the indenyl ligands at and below room temperature for **1** and its dichloro analogue, (2-PhInd)$_2$ZrCl$_2$, with the substitution pattern of the ligands playing a major role in determining the rotation rate. For example, the rate constant k_r for the isomerization of (2-PhInd)$_2$ZrMe$_2$ **1** was 14 000 ± 4500 s^{-1} at −121 °C, the rate constant for the dibenzyl analogue, (2-PhInd)$_2$ZrBn$_2$, approaches this value only at 25 °C (k_r = 24 000 ± 4300 s^{-1}).[18] Modifying the indenyl framework has a similar if less pronounced effect (k_r for (2-(3′,5′-di-*tert*-butyl)PhInd)$_2$ZrBn$_2$ at 89 °C = 11 700 ± 3000 s^{-1}).

For (2-PhInd)$_2$ZrBn$_2$,[21] (2-phenylcyclopenta[1]phenanthrene)$_2$ZrBn$_2$,[19] and (2-aminoindenyl)$_2$ZrCl$_2$ complexes,[22] dynamic NMR studies implicate the rapid interconversion of two enantiomeric *anti* conformers at low temperatures; these studies provided no evidence for the achiral *syn* isomer in solution. This is consistent with calculations that imply that the *anti* conformers are slightly lower in energy; however for the dibenzyl derivatives, it may also be a consequence of the preference of the two benzyl groups to adopt an *anti* conformation, thereby stabilizing the *anti* configuration of the two arylindene ligands. The steric demands of the two benzyl groups might also interfere with π-stacking of the phenyl ligands,[23] which was proposed to play a significant role in stabilizing the *syn* conformer.[5,6] In any case, the results of the dynamic NMR studies for the neutral metallocenes imply that the conformational dynamics are much too fast to be competitive with reasonable estimates for the monomer insertion rates (approximately 10−100 insertions s^{-1}).[2,9]

It is important to emphasize that the neutral catalyst precursor (**1**) and the actively polymerizing cationic species differ significantly both structurally and electronically, and their conformational dynamics cannot be assumed to be the same. The catalyst precursor is neutral and relatively sterically unhindered. The active catalyst is cationic, ligated by the growing polymer chain, and associated with a counteranion; the latter two features are likely to influence the catalyst's conformational dynamics. In fact, Busico had proposed that the close association of B(C$_6$F$_5$)$_4^-$ anions in nonpolar solvents leads to the stabilization of chiral *anti* conformations (the "locked-rac" hypothesis), which are responsible for the generation of long isotactic sequences in these metallocenes.[9] Thus, it is clear that a better understanding of the accessible conformations requires an understanding of the interplay between ion-pairing dynamics[24−30] and conformational dynamics.

In this work, we sought to examine cationic 2-arylindene metallocenes that might provide more appropriate models for active catalysts; in particular we report NMR investigations of a series of 2-arylindene zirconocene methyl cations (**2a**,**b**) and cationic zirconocenium-pyridyl complexes (**3a**−**8b**, Scheme 2). The pyridyl complexes are generated by activation of **1** with B(C$_6$F$_5$)$_3$ or [Ph$_3$C$^+$][B(C$_6$F$_5$)$_4^-$] and subsequent reaction with *o*-substituted pyridines, eliminating methane.[31] They approximate an actively polymerizing zirconocene catalyst in several key aspects: the complexes have been activated by typical polymerization cocatalysts, possess cationic metal centers, and have ligands that bring steric bulk proximate to the metal center similar to that of a growing polymer chain (Scheme 3). We here describe a series of variable-temperature one- and two-dimensional ^{1}H, ^{13}C, and ^{19}F NMR experiments carried out in order to estimate the activation parameters for

(18) Wilmes, G. M.; France, M. B.; Lynch, S. R.; Waymouth, R. M. *Organometallics* **2004**, *23*, 2405−2411.
(19) Schneider, N.; Schaper, F.; Schmidt, K.; Kirsten, R.; Geyer, A.; Brintzinger, H. H. *Organometallics* **2000**, *19*, 3597−3604.
(20) Dreier, T.; Bergander, K.; Wegelius, E.; Frohlich, R.; Erker, G. *Organometallics* **2001**, *20*, 5067−5075.
(21) Bruce, M. D.; Coates, G. W.; Hauptman, E.; Waymouth, R. M.; Ziller, J. W. *J. Am. Chem. Soc.* **1997**, *119*, 11174−11182.
(22) Dietrich, U.; Hackmann, M.; Rieger, B.; Klinga, M.; Leskela, M. *J. Am. Chem. Soc.* **1999**, *121*, 4348−4355.
(23) Deck, P. A.; Kroll, C. E.; Hollis, W. G.; Fronczek, F. R. *J. Organomet. Chem.* **2001**, *637*, 107−115.
(24) Zuccaccia, C.; Stahl, N. G.; Macchioni, A.; Chen, M. C.; Roberts, J. A.; Marks, T. J. *J. Am. Chem. Soc.* **2004**, *126*, 1448−1464.
(25) Chen, M. C.; Roberts, J. A. S.; Marks, T. J. *J. Am. Chem. Soc.* **2004**, *126*, 4605−4625.
(26) Stahl, N. G.; Zuccaccia, C.; Jensen, T. R.; Marks, T. J. *J. Am. Chem. Soc.* **2003**, *125*, 5256−5257.
(27) Chen, M. C.; Marks, T. J. *J. Am. Chem. Soc.* **2001**, *123*, 11803−11804.
(28) Deck, P. A.; Marks, T. J. *J. Am. Chem. Soc.* **1995**, *117*, 6128−6129.
(29) Guo, Z. Y.; Swenson, D. C.; Jordan, R. F. *Organometallics* **1994**, *13*, 1424−1432.
(30) Bochmann, M.; Lancaster, S. J. *Angew. Chem., Int. Ed. Engl.* **1994**, *33*, 1634−1637.
(31) Dagorne, S.; Rodewald, S.; Jordan, R. F. *Organometallics* **1997**, *16*, 5541−5555.

Scheme 2. Bis(2-phenylindenyl)zirconocene Complexes Studied

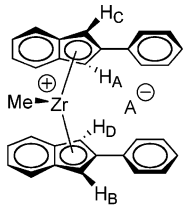

Compound	A^-
2a	$[CH_3B(C_6F_5)_3^-]$
2b	$[B(C_6F_5)_4^-]$

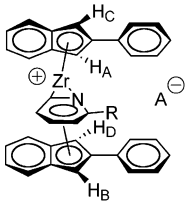

Compound	R	A^-
3a	H	$[CH_3B(C_6F_5)_3^-]$
3b	H	$[B(C_6F_5)_4^-]$
4a	Me	$[CH_3B(C_6F_5)_3^-]$
4b	Me	$[B(C_6F_5)_4^-]$
5a	Et	$[CH_3B(C_6F_5)_3^-]$
5b	Et	$[B(C_6F_5)_4^-]$
6a	^{i}Pr	$[CH_3B(C_6F_5)_3^-]$
6b	^{i}Pr	$[B(C_6F_5)_4^-]$
7a	^{t}Bu	$[CH_3B(C_6F_5)_3^-]$
7b	^{t}Bu	$[B(C_6F_5)_4^-]$
8a	CH_2Ph	$[CH_3B(C_6F_5)_3^-]$
8b	CH_2Ph	$[B(C_6F_5)_4^-]$

Scheme 3. Steric and Electronic Similarities between the Pyridyl Model Complexes and an Actively Polymerizing Zirconocene Catalyst

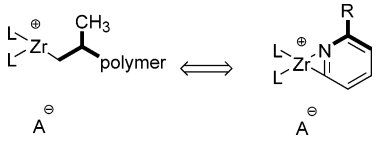

the relevant processes of ion-pair separation and dissociation−reassociation for catalysts **2a** and **2b** and studies that reveal the presence of achiral *syn* conformations of zirconocenium-pyridyl complexes in solution.

Results and Discussion

Variable-Temperature Behavior of 1, 2a, and 2b. The unbridged metallocene **1** was prepared by a slight modification of the literature procedure.[1] Treatment of **1** with $B(C_6F_5)_3$ (**B2**) or $[Ph_3C^+][B(C_6F_5)_4^-]$ (**B4**) at room temperature cleanly generated $[(2\text{-PhInd})_2ZrMe^+][MeB(C_6F_5)_3^-]$ (**2a**) or $[(2\text{-PhInd})_2ZrMe^+][B(C_6F_5)_4^-]$ (**2b**), respectively, within minutes as determined by ^1H and ^{13}C NMR spectroscopy in C_6D_5Cl.

The dynamic behavior of the neutral metallocene **1** was evaluated over the temperature range −40 to 100 °C in 10 °C increments and compared to that of the cation−anion pairs **2a** and **2b**. In this temperature range, the ^1H NMR spectrum of **1** exhibits a singlet (4H) at ∼6.0 ppm for the cyclopentadienyl (Cp) protons and a singlet (3H) at ∼ −1.0 ppm for the Zr-CH_3 protons. These observations are consistent with the known rapid rotation of the indenyl ligands in this temperature range.[18]

In d_8-toluene at 100 °C, the ^1H NMR spectrum of **2a** exhibits one singlet for the cyclopentadienyl protons at

Scheme 4. Intramolecular $B(C_6F_5)_3$ (k_{dr}) and $[MeB(C_6F_5)_3-]$ (k_{Ips}) Exchange Processes in 2a

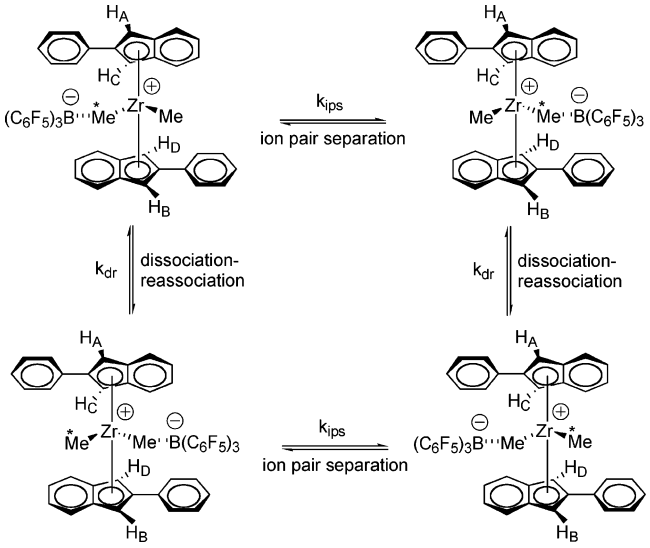

6.12 ppm and a singlet for the Zr-CH_3 protons at −0.30 ppm. As the temperature is decreased, the cyclopentadienyl resonances broaden and decoalesce. At −40 °C, complex **2a** shows two singlets arising from the cyclopentadienyl protons (δ = 5.94 ppm, 5.65 ppm, 2H each), a sharp singlet from the Zr-CH_3 protons (δ = −0.29 ppm), and a quadrupolar-broadened singlet from the methyl group bridging the zirconocenium cation and the borate anion (δ = −0.58 ppm), consistent with a zirconium-bound C$H_3B(C_6F_5)_3^-$. A small singlet from C$H_3B(C_6F_5)_3^-$ (δ =1.35 ppm) was also observed. These observations indicate the occurrence of one or more dynamic processes, which we attribute to ion-pair dynamics coupled with rotation of the indenyl ligands in analogy with the work of Marks on related metallocenes.[28,32−35]

The variable-temperature ^1H NMR spectra of **2a** are most consistent with rapid ligand rotation coupled to two ion-pair exchange processes: (1) an ion-pair symmetrization process, characterized by the rate constant k_{ips} in which the C$H_3B(C_6F_5)_3^-$ anion reversibly associates at the two diastereotopic coordination sites, and (2) the reversible association of $B(C_6F_5)_3$ to the two Zr-CH_3 groups, characterized by the rate constant k_{dr} (Scheme 4).[33] The first process is characterized by exchange of cyclopentadienyl protons H_A and H_B and of H_C and H_D (Scheme 2). Reversible association of $B(C_6F_5)_3$ exchanges not only the cyclopentadienyl protons but also the two Zr-CH_3 protons.

The rate constants and activation energies of ion-pair separation and $MeB(C_6F_5)_3^-$ dissociation−reassociation were determined by line-shape analysis of the spectra (Table 1). The enthalpy and entropy of activation for ion-pair separation were found by least-squares fitting of an Eyring plot to be $\Delta H^{\ddagger}_{ips} = 20 \pm 1$ kcal/mol and $\Delta S^{\ddagger}_{ips} = 17 \pm 4$ eu. The rate of ion-pair separation was

(32) Yang, X. M.; Stern, C. L.; Marks, T. J. *J. Am. Chem. Soc.* **1991**, *113*, 3623−3625.
(33) Yang, X. M.; Stern, C. L.; Marks, T. J. *J. Am. Chem. Soc.* **1994**, *116*, 10015−10031.
(34) Deck, P. A.; Beswick, C. L.; Marks, T. J. *J. Am. Chem. Soc.* **1998**, *120*, 1772−1784.
(35) Deck, P. A.; Beswick, C. L.; Marks, T. J. *J. Am. Chem. Soc.* **1998**, *120*, 12167.

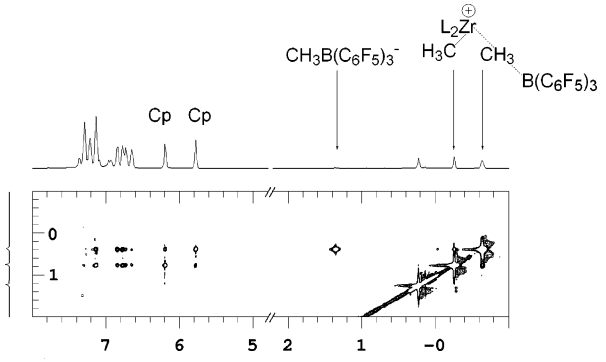

Figure 1. Room-temperature ^{1}H−^{1}H NOESY spectrum for **2a** in C_6D_5Cl.

Table 1. Kinetic Data for Ion-Pair Reorganization Processes of 2a in d_8-Toluene

T (°C)	k_{ips} (s^{-1})	$\Delta G^{\ddagger}_{ips}$ (kcal/mol)	k_{dr} (s^{-1})	$\Delta G^{\ddagger}_{dr}$ (kcal/mol)
0 ± 0.5	6 ± 1	15.0 ± 0.1		
10	20 ± 1	14.9		
24	80 ± 4	14.8		
34	300 ± 14	14.5		
44	900 ± 50	14.3		
55	3,000 ± 150	14.0		
64	8,600 ± 430	13.7	24 ± 1	17.8 ± 0.1
73	18,000 ± 900	13.6	46 ± 2	18.4
83	27,000 ± 1,400	13.7	78 ± 4	18.9
98	68,000 ± 3,400	13.7	160 ± 8	19.8

much faster than the rate of $B(C_6F_5)_3$ dissociation, but the temperature range we could access with these experiments precluded a reliable estimation of the activation parameters for reversible association of $B(C_6F_5)_3$. Both processes occurred more rapidly ($k_{ips,T=83°C}$ = 27 000 s^{-1}, $\Delta G^{\ddagger}_{ips,T=83°C}$ = 13.7 kcal/mol; $k_{dr,T=83°C}$ = 78 s^{-1}, $\Delta G^{\ddagger}_{dr,T=83°C}$ = 18.9 kcal/mol) than those observed in the compound $[(1,2\text{-}Me_2Cp)_2ZrMe^+][MeB(C_6F_5)_3^-]$, for which Marks calculated k_{ips} = 30 s^{-1} and k_{dr} = 4 s^{-1} at 80 °C with $\Delta H^{\ddagger}_{ips}$ = 24 ± 1 kcal/mol and $\Delta S^{\ddagger}_{ips}$ = 17 ± 2 eu ($\Delta G^{\ddagger}_{ips,T=80°C}$ = 18.3 kcal/mol, $\Delta G^{\ddagger}_{dr,T=80°C}$ = 19.7 kcal/mol).[33] Sieldle and Newmark reported similar dynamics for $[(Ind)_2ZrMe^+][MeB(C_6F_5)_3^-]$ with $\Delta G^{\ddagger}_{ips}$ = 15.8 kcal/mol and $\Delta G^{\ddagger}_{dr}$ = 18.1 kcal/mol.[36]

Further evidence for ion-pair separation was obtained from the low-temperature (−40 °C) NOESY spectrum of complex **2a** (Figure 1) in C_6D_5Cl. This spectrum reveals a cross-peak between the Zr-CH_3 resonance at δ = −0.58 ppm and the free CH_3B$(C_6F_5)_3^-$ resonance at 1.35 ppm, consistent with exchange between free and bound CH_3B$(C_6F_5)_3^-$. Moreover, the cross-peaks between both cyclopentadienyl protons and both the CH_3B$(C_6F_5)_3^-$ resonances and the Zr-CH_3 resonances indicate that rotation of the indenyl ligands remains rapid at −40 °C.

The room-temperature spectrum of the ion pair **2b** in a 1:1 mixture of d_5-chlorobenzene and d_8-toluene shows one cyclopentadienyl singlet (δ = 6.01 ppm) and one Zr-Me singlet (δ = −0.32 ppm). Below −30 °C, the cyclopentadienyl resonance decoalesces into two singlets (T = −50 °C: δ = 6.15, 5.66 ppm). Line-shape analysis was used to determine the activation energies of this phenomenon (Table 2). The enthalpy and entropy of activation were determined to be $\Delta H^{\ddagger}_{ips}$ = 15 ± 2 kcal/mol and $\Delta S^{\ddagger}_{ips}$ = 13 ± 7 eu. The observed dynamic behavior is consistent with the reversible coordination of either the $[B(C_6F_5)_4^-]$ anion or a solvent molecule.[37,38] Variable-temperature ^{19}F NMR studies of **2b** in chlorobenzene show slight broadening of the *para*-fluoro resonance (δ = −162.5 ppm) upon cooling from room temperature to −40 °C, which is suggestive but not definitive evidence of reversible association of the $[B(C_6F_5)_4^-]$ anion. The lower activation barriers for the ion-pair dynamics for the $[B(C_6F_5)_4^-]$ anion are in agreement with previous observations that $B(C_6F_5)_4^-$ coordinates more weakly than the $MeB(C_6F_5)_3^-$ anion to zirconocene cations. These observations are also consistent with our[39] and others'[17] observations that catalysts derived from the $MeB(C_6F_5)_3^-$ anions exhibit much lower activities in olefin polymerization. Moreover, NMR analysis of metallocene cations **2a** and **2b** provides no evidence that the association of the anions with the $(2\text{-PhInd})_2ZrMe^+$ cations leads to locked conformations at temperatures above −40 °C.

Table 2. Kinetic Data for Ion-Pair Reorganization Processes of 2b in d_8-Toluene/d_5-Chlorobenzene

T (°C)	k (s^{-1})	$\Delta G^{\ddagger}$ (kcal/mol)
−58 ± 0.5	5 ± 1	11.81 ± 0.07
−48	16 ± 1	11.81 ± 0.04
−39	63 ± 3	11.69 ± 0.03
−29	360 ± 60	11.34 ± 0.09
−19	970 ± 250	11.31 ± 0.13
0	7200 ± 2200	11.13 ± 0.17
20	31 000 ± 14 000	11.11 ± 0.25

Synthesis of Zirconocenium-Pyridyl Complexes. While the zirconocenium methyl cations provide good models for the initiating species in olefin polymerization, they are not good models for the catalytic species responsible for propagation, as the growing polymer chain is likely to be important for its influence both on stereodifferentiation of monomer insertion[40−43] and on the ligand rotation dynamics.[18] As we had previously observed that the nature of the zirconium-alkyls have a significant influence on the rotation dynamics of the indenyl ligands, we sought more sterically hindered cations that might be more representative of a steric environment featuring a growing polymer chain. For this reason, we were attracted to the work of Jordan, who demonstrated that pyridines react rapidly with zirconocene cations to provide stable η^2-coordinated pyridine adducts.[31]

At room temperature, the reaction of **2a** or **2b** with a variety of *ortho*-substituted pyridines in C_6D_5Cl rapidly generates methane and $[(2\text{-PhInd})_2Zr(2\text{-R-pyridyl})^+][MeB(C_6F_5)_3^-]$ or $[(2\text{-PhInd})_2Zr(2\text{-R-pyridyl})^+][B(C_6F_5)_4^-]$, respectively, for R = H, Me, Et, iPr, Bn, tBu.[44]

For **2a**, coordination of 2-isopropylpyridine is rapid at room temperature, as evidenced by the immediate

(36) Siedle, A. R.; Newmark, R. A. *J. Organomet. Chem.* **1995**, *497*, 119−125.

(37) Jia, L.; Yang, X. M.; Stern, C. L.; Marks, T. J. *Organometallics* **1997**, *16*, 842−857.

(38) Stoebenau, E. J.; Jordan, R. F. *J. Am. Chem. Soc.* **2003**, *125*, 3222−3223.

(39) Wilmes, G. M.; Polse, J. L.; Waymouth, R. M. *Macromolecules* **2002**, *35*, 6766−6772.

(40) Guerra, G.; Cavallo, L.; Moscardi, G.; Vacatello, M.; Corradini, P. *Macromolecules* **1996**, *29*, 4834−4845.

(41) Cavallo, L.; Guerra, G.; Corradini, P. *J. Am. Chem. Soc.* **1998**, *120*, 2428−2436.

(42) Milano, G.; Fiorello, G.; Guerra, G.; Cavallo, L. *Macromol. Chem. Phys.* **2002**, *203*, 1564−1572.

(43) Minieri, G.; Corradini, P.; Guerra, G.; Zambelli, A.; Cavallo, L. *Macromolecules* **2001**, *34*, 5379−5385.

Scheme 5. Proposed Reaction Observed on Addition of *o*-Isopropylpyridine to 2a

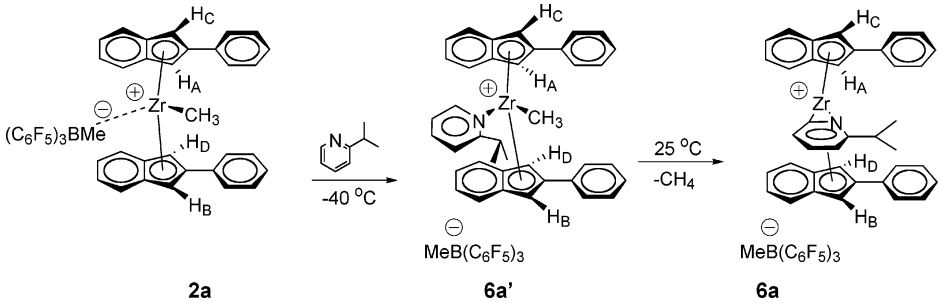

appearance of a Zr-CH_3 singlet at 0.18 ppm, two cyclopentadienyl singlets at 6.20 and 5.68 ppm, a broad singlet at 8.40 ppm due to the *ortho*-proton of the zirconium-bound pyridine, and a resonance (d, 6H) for the isopropyl methyl groups at 0.73 ppm. At room temperature, the subsequent elimination of methane (δ = 0.10 ppm) could be monitored by ^{1}H NMR over approximately 30 min to give the η^2-coordinated 2-isopropylpyridyl adduct characterized by two cyclopentadienyl resonances at 6.02 and 5.82 ppm and a resonance (d, 6H) for the isopropyl methyl groups at 0.81 ppm (Scheme 5).

Variable-Temperature Behavior of Zirconocenium-Pyridyl Complexes. The temperature-dependent behavior of the pyridyl complexes **3a**−**8b** was explored by ^{1}H NMR spectroscopy between −40 and 100 °C in C_6D_5Cl. At 100 °C, the spectra of the protio-, methyl-, ethyl-, isopropyl-, *tert*-butyl-, and benzyl-pyridyl complexes each exhibit two cyclopentadienyl proton singlets at roughly 6 and 5.8 ppm. Below 100 °C, the two cyclopentadienyl resonances of **3a**−**8b** exhibit striking asymmetric temperature-dependent chemical shifts: the upfield cyclopentadienyl resonance moves slightly downfield, whereas the downfield cyclopentadienyl resonance moves significantly upfield (e.g., Figure 2). The temperature at which the cyclopentadienyl proton resonances cross one another follows a steric trend, specifically **3a**,**b** (50−60 °C), **4a**,**b** (20 °C), **5a**,**b** (0 °C), **6a**,**b** (−10 °C), and **7a**,**b** and **8a**,**b** (do not overlap as low as −40 °C). At low temperature (between −30 and −40 °C), the methyl- and isopropyl-pyridyl complexes undergo noticeably asymmetric broadening of their upfield cyclopentadienyl signals, while their downfield cyclopentadienyl signals remain sharp. These observations suggest the electronic environments of the cyclopentadienyl protons differ markedly as the temperature is decreased to −40 °C.

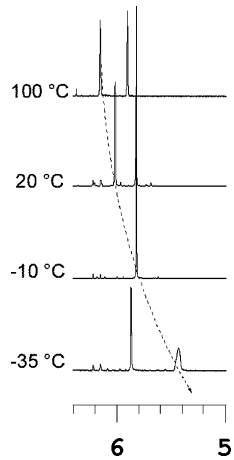

Figure 2. Variable-temperature ^{1}H NMR showing the cyclopentadienyl resonances for compound **6a** between −35 and 100 °C in C_6D_5Cl.

Variable-temperature (−40 to −90 °C) ^{1}H NMR spectra of the methylpyridine complex **4a** in $CDCl_2F$[45] yield similar temperature-dependent chemical shifts for the cyclopentadienyl resonances, but the temperature at which the cyclopentadienyl resonances cross over is lower for **4a** in $CDCl_2F$ (−40 °C) than in chlorobenzene (20 °C). Thus, the crossover temperature is sensitive not only to the steric demands of the substituent on the pyridine ligand but also to the nature of the solvent.[28]

The observation of two cyclopentadienyl resonances in the low-temperature spectra of the pyridine complexes **3a**−**8b** and the observation of a single resonance for the isopropyl methyl groups for **6a**,**b** at all temperatures suggests either that rotation of the phenylindenyl ligands is rapid (time-averaged C_s symmetry) or that only one C_s-symmetric *syn* conformer predominates at low temperature.

To provide further information about the conformational behavior of these cationic pyridyl complexes, a series of variable-temperature 2D ^{1}H/^{1}H NOESY experiments were performed (Figure 3). The room-temperature NOESY spectrum of the isopropylpyridyl complex **6a** in d_5-chlorobenzene shows a correlation of the isopropyl CH_3 proton resonance to both cyclopentadienyl proton resonances. No correlation is seen between the cyclopentadienyl resonances and the isopropyl C*H* proton. These observations are most consistent with rapid phenylindenyl ligand rotation at room temperature. In contrast, the NOESY spectrum of **6a** at −35 °C shows strong correlation between the isopropyl CH_3 protons and only the sharper downfield cyclopentadienyl resonance. A weaker correlation is also seen between the downfield cyclopentadienyl resonance and the isopropyl C*H* proton at 2.15 ppm.[46] Thus, the correlation

(44) Pyridine-B(C_6F_5)$_3$ adducts are also generated in trace amounts. Interestingly, the borane adducts of the ethyl-, isopropyl-, and benzylpyridines exhibit restricted rotation; the ethyl CH_2 resonance is a diastereotopic doublet of multiplets (2.67 and 62.80 ppm), the isopropyl CH_3 resonances are a doublet of doublets (60.13 and 61.04 ppm), and the benzyl CH_2 resonance is a doublet of doublets (64.15 and 64.45 ppm). Such restricted rotation is not observed for the zirconocenium-pyridyl complexes.

(45) Siegel, J. S.; Anet, F. A. L. *J. Org. Chem.* **1988**, *53*, 2629−2630.

(46) It is possible that the breadth of the upfield cyclopentadienyl resonance might cause similar broadening in the NOE cross-peak such that a correlation may not be observed even if both cyclopentadienyl resonances experience correlation with the isopropyl methyl resonance. However, the broad upfield cyclopentadienyl resonance exhibits correlation to other resonances with a strength comparable to the downfield cyclopentadienyl resonance; for example, both cyclopentadienyl proton resonances correlate to a signal at 7.0 ppm (the proton of the phenyl protons nearest in space to the cyclopentadienyl protons).

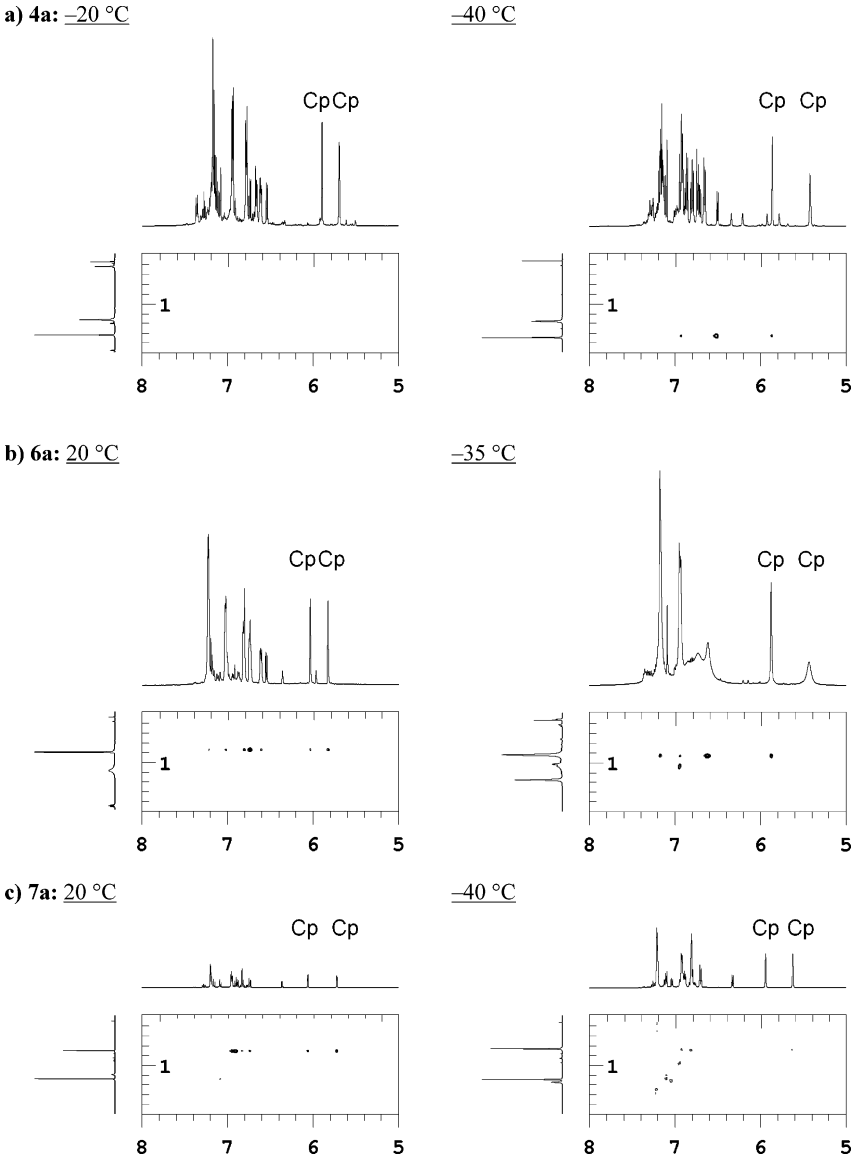

Figure 3. Room-temperature and low-temperature $^1H-^1H$ NOESY spectra for the (a) methyl, (b) isopropyl, and (c) *tert*-butyl complexes in C_6D_5Cl.

between only one of the cyclopentadienyl resonances with resonances corresponding to the pyridine isopropyl resonances indicates that at −35 °C rotation of the indenyl ligands is slow and leads to the predominance of a single *syn* conformer. As this is one of the first indications of the presence of a *syn* isomer in solution, we sought to confirm these observations for the related methylpyridyl complex **4a** and the *tert*-butylpyridyl complex **7a**.

For the methylpyridyl complex **4a**, the cyclopentadienyl resonances have nearly identical chemical shifts at room temperature, which precludes carrying out an analogous NOESY experiment at this temperature. At −20 °C, the NOESY spectrum of **4a** shows no NOE transfer between the cyclopentadienyl resonances and the pyridyl methyl resonance (Figure 3). Presumably, at this temperature the dynamics of the indenyl ligands are such that the cyclopentadienyl protons and methyl protons are not held in close proximity for a time sufficient for efficient NOE transfer. However, at −40 °C, the NOESY spectrum of **4a** shows correlation between the pyridyl CH_3 protons and only the downfield cyclopentadienyl resonance, consistent with the predominance of only one *syn* conformer.[47] This is consistent with the observation of a correlation between the isopropyl methyl resonances of **6a** (vide supra) at −40 °C but not at room temperature. Closer inspection of the −40 °C NOESY spectrum of **4a** (Supporting Information) reveals a correlation between the pyridine methyl resonances at 1.75 ppm and the *ortho* protons of the phenyl group at 6.90 ppm (Figure 3), implicating that the predominant *syn* isomer is that which positions the 2-phenyl and methyl substituents in close proximity (Scheme 2).

The variable-temperature NMR spectra of the *tert*-butyl-substituted pyridine complexes **7a** and **7b** are slightly different than those of their less sterically hindered congeners; in contrast to the variable-temperature behavior of complexes **3a**−**6b**, the cyclopentadienyl proton signals for the *tert*-butyl complexes **7a** and **7b** exhibit temperature-dependent chemical shifts but do not cross over in the temperature range studied. Nevertheless, the NOESY spectrum of **7a** shows a

(47) As for **6a**, the strength of the cross-peaks observed for both cyclopentadienyl protons to the phenyl ring protons was similar.

correlation between the *tert*-butyl resonance and both cyclopentadienyl resonances at room temperature, whereas the *tert*-butyl resonance shows a correlation to only the upfield cyclopentadienyl resonance at −40 °C (Figure 3). At this temperature, a correlation analogous to that observed in the low-temperature **6a** NOESY spectrum is observed between the *tert*-butyl protons and the *ortho* protons of the 2-phenyl substituent, again suggesting that the predominant *syn* isomer holds these groups in close proximity.

Finally, to better characterize the $[(2\text{-PhInd})_2ZrMe\text{-}(2\text{-iPr-pyridine})^+][MeB(C_6F_5)_3^-]$ intermediate (**6a′**), 2-isopropylpyridine was added to **2a** at −40 °C and a NOESY experiment was performed prior to the elimination of methane to generate **6a**. This spectrum reveals a correlation between the Zr-CH_3 resonance at 0.20 ppm and both cyclopentadienyl resonances, and a correlation between both the isopropylpyridine methyl resonance ($\delta = 0.70$ ppm) and methine resonance ($\delta = 1.07$ ppm) and only the downfield cyclopentadienyl resonance($\delta =$ 6.14 ppm) (Figure 3). Such behavior is also consistent with the presence of only one *syn* conformer.

Thus, the low-temperature NOESY spectra of the cations **4a**, **6a**, **6a′**, and **7a** reveal that 2-phenylindene metallocene cations ligated by cyclometalated 2-alkyl pyridines exist primarily as the achiral *syn* conformers at −40 °C. These results imply that the achiral *syn* isomers are accessible conformations not only in the solid state[1] but also in solution. Moreover these results suggest that the nature of the accessible conformations of these conformationally dynamic catalysts is a complicated function of the nature of the arylindene ligands, the cation/anion interactions, and the nature of the alkyl group bound to the metallocene cation.

Conclusions

NMR investigations of conformationally dynamic unbridged zirconocenium methyl cations $[(2\text{-PhInd})_2ZrMe^+][RB(C_6F_5)_3^-]$ (R = Me, C_6F_5) reveal that association of sterically hindered counterions $[RB(C_6F_5)_3^-]$ does not provide a sufficient steric barrier to inhibit the conformational dynamics of the 2-arylindene ligands. No evidence was found that suggests the association of the anions with the $(2\text{-PhInd})_2ZrMe^+$ cations leads to "locked" conformations at temperatures above −40 °C. The activation barrier for ion-pair separation of the zirconocene cations and $RB(C_6F_5)_3^-$ was shown to be slightly higher but in the range observed for related zirconocene methyl cations. The higher activation barriers for ion-pair separation of $CH_3B(C_6F_5)_3^-$ relative to $B(C_6F_5)_4^-$ are consistent with polymerization data that indicate the $B(C_6F_5)_4^-$ anion coordinates more weakly to the metal center than the $CH_3B(C_6F_5)_3^-$ anion, leading to higher productivities.

Cationic *o*-substituted pyridyl complexes were prepared as steric analogues to active cationic species ligated to a growing polymer chain. Low-temperature NOESY spectra of the cyclometalated pyridine zirconocene cations provide the first evidence for the presence of C_s-symmetric *syn* conformations in solution.

Experimental Section

General Procedures. Standard Schlenk techniques and a Vacuum Atmospheres drybox were used to handle air- and moisture-sensitive compounds. Dichlorofluoromethane[45] and 2-isopropylpyridine[48] were synthesized according to the literature procedures. Dichlorofluoromethane, all pyridines used, d_5-chlorobenzene (Fisher), and d_8-toluene were stirred over calcium hydride for at least 6 h under a nitrogen blanket and distilled and degassed prior to use. Tris(pentafluorophenyl)-borane and trityl tetrakis(pentafluorophenyl)borate (Strem) were used as delivered. All chemicals were obtained from Aldrich unless otherwise noted.

Synthesis of (2-Phenylindenyl)$_2$ZrMe$_2$. The compound was prepared following a slight modification of the literature procedure reported by Coates and Resconi.[1,49] Methyllithium (24.0 mL, 1.6 M in diethyl ether, 38.4 mmol) was added dropwise to a stirred solution of 2-phenylindene (3.85 g, 20.0 mmol) in 250 mL of diethyl ether at −78 °C. The resulting dark brown solution was allowed to warm to room temperature and stirred in the dark for 12 h. The solution was then transferred to a suspension of zirconium tetrachloride (2.55 g, 11.0 mmol) in 50 mL of pentane. When the lighter brown solution began to darken after 1 h, the solvent was removed in vacuo, leaving a dark brown residue. The product was dissolved in toluene, filtered through Celite, and concentrated in vacuo to 50 mL. The product crystallized from this solution at −50 °C as a pale yellow solid (3.3 g, 6.5 mmol, 65% yield). ^{1}H NMR (C_6D_6, 500 MHz): δ (ppm) 7.31 (d, $J = 0.01$ Hz, 4H), 7.20 (d, $J = 0.01$ Hz, 4H), 7.10 (t, $J = 0.02$ Hz, 2H), 7.04 (q, $J = 0.08$ Hz, 4H), 6.94 (q, $J = 0.08$ Hz, 4H), 6.90 (t, $J = 0.10$ Hz, 4H), 5.96 (s, 4H, Cp), −1.05 (s, 6H, Zr-CH_3).

Preparation of Methyl Cations. Compounds **2a** and **2b** were prepared for NMR analysis as follows. Under nitrogen, both **1** and $B(C_6F_5)_3$ or $[Ph_3C^+][B(C_6F_5)_4^-]$ were weighed directly into a 5 mm Teflon-capped (J. Young) NMR tube, dissolved in C_6D_5Cl, and allowed to react for at least 20 min prior to use in NMR experiments unless otherwise indicated. The rate of decomposition of the methyl cations has prevented their characterization by elemental analysis or X-ray crystallography. The methyl cations have also proven insufficiently stable toward appropriate solvents to permit characterization by mass spectroscopy. In lieu of such analyses, the ^{1}H NMR spectra of **2a** and **2b** at room temperature and below are included in the Supporting Information, and their ^{1}H and ^{13}C chemical shifts are recorded in Tables 3 and 4.

Preparation of Zirconocenium Pyridyl Cations. The *o*-substituted pyridyl cations **3a**−**8b** were prepared for NMR analysis as follows. Under nitrogen, stock solutions of pyridine or 2-alkylpyridines (∼50 mg/1 mL C_6D_5Cl) were prepared, and slightly less than 1 equiv was added by micropipet to a Teflon-capped (J. Young) NMR tube containing the appropriate methyl cation (**2a** or **2b**) in C_6D_5Cl. The sample was allowed to react for at least 20 min prior to use in NMR experiments unless otherwise indicated. When preparing the pyridyl, methylpyridyl, and ethylpyridyl complexes, slightly less than 1 equiv of the pyridine was used, as these complexes are prone to coordination of a second equivalent of pyridine; in the ^{1}H NMR spectra, this slight imbalance is manifested in resonances near −0.2 ppm due to $[(2\text{-PhInd})_2ZrCH_3^+][MeB(C_6F_5)_3^-]$ and near −0.6 ppm due to $[(2\text{-PhInd})_2Zr^+\text{-}\text{-}CH_3\text{-}\text{-}^-MeB(C_6F_5)_3]$. Attempts to isolate the pyridyl complexes produce oils from which solvent cannot be removed completely; their characterization by elemental analysis or X-ray crystallography has thus been prevented. The pyridyl cations have also proven insufficiently stable toward appropriate solvents to permit characterization by mass spectroscopy. In lieu of such analyses, the room-temperature ^{1}H NMR chemical shifts of **3a**−**8a** are recorded in Table 3, and for the representative complexes **4a**, **6a**, and **7a**, the room-temperature ^{13}C NMR chemical shifts

(48) Pasquinet, E.; Rocca, P.; Marsais, F.; Godard, A.; Queguiner, G. *Tetrahedron* **1998**, *54*, 8771−8782.
(49) Balboni, D.; Camurati, I.; Prini, G.; Resconi, L.; Galli, S.; Mercandelli, P.; Sironi, A. *Inorg. Chem.* **2001**, *40*, 6588−6597.

Table 3. Room-Temperature ^{1}H NMR Chemical Shifts for 1, 2a, 2b, and 3a−8a (500 MHz, C_6D_5Cl)

	δ (ppm)	multiplicity	integration	assignment
1	−1.05	s	3	$ZrCH_3$
	5.96	s	4	Cp
	6.85−7.35	m	18	Ar−H
2a	−0.37	bs	3	$ZrCH_3$
	−0.37	s	3	$CH_3B(C_6F_5)_3^-$
	6.10	bs	4	Cp
	6.65−7.45	m	18	Ar-H
2b	−0.28	s	3	$ZrCH_3$
	1.97	s	3	Ph_3CMe
	6.09	s	4	Cp
	6.65−7.45	m	18	Ar-H
3a	0.10	s	4	CH_4
	1.18	s	3	$CH_3B(C_6F_5)_3^-$
	5.87	d (J = 2.4 Hz)	2	Cp
	6.23	d (J = 2.4 Hz)	2	Cp
	6.55−7.80	m	21	Ar-H
4a	0.10	s	4	CH_4
	1.19	bs	3	$CH_3B(C_6F_5)_3^-$
	1.56	s	3	CH_3
	5.98	qd (J_1 = 2.4 Hz, J_2 = 0.7 Hz)	4	Cp
	6.50−7.35	m	21	Ar-H
5a	0.10	s	4	CH_4
	0.79	t (J = 7.6 Hz)	3	CH_3
	1.21	s	3	$CH_3B(C_6F_5)_3^-$
	1.85	q (J = 7.4 Hz)	2	CH_2
	5.88	d (J = 2.05 Hz)	2	Cp
	5.95	bs	2	Cp
	6.50−7.40	m	21	Ar-H
6a	0.10	s	4	CH_4
	0.81	d (J = 7.0 Hz)	6	iPr CH_3
	1.21	s	3	$CH_3B(C_6F_5)_3^-$
	1.92	sept (J = 7.0 Hz)	1	iPr CH
	5.82	d (J = 2.1 Hz)	2	Cp
	6.02	d (J = 2.1 Hz)	2	Cp
	6.50−7.35	m	21	Ar-H
7a	0.10	s	4	CH_4
	1.20	s	3	$CH_3B(C_6F_5)_3^-$
	1.29	s	9	tBu CH_3
	5.70	dd (J_1 = 7.8 Hz, J_2 = 0.7 Hz)	2	Cp
	6.04	dd (J_1 = 2.4 Hz, J_2 = 0.5 Hz)	2	Cp
	6.30	dd (J_1 = 2.4 Hz, J_2 = 0.9 Hz)	1	Ar-H
	6.70−7.30	m	21	Ar-H
8a	0.10	s	4	CH_4
	1.22	s	3	$CH_3B(C_6F_5)_3^-$
	3.22	s	2	CH_2
	5.30	bs	2	Cp
	5.69	d (J = 1.8 Hz)	2	Cp
	5.85−7.65	m	26	Ar-H

are recorded in Table 4; ^{1}H NMR spectra at and below room temperature are also included for **4a**, **6a**, and **7a** in the Supporting Information.

Variable-Temperature ^{1}H NMR. Samples for use in variable-temperature ^{1}H NMR experiments were prepared as above. Spectra were recorded on either a Varian Unity Inova 300 MHz NMR spectrometer equipped with a 5 mm broadband switchable probe, a Varian Mercury AS400 MHz NMR equipped with a 5 mm 4-nucleus (^{13}C/^{31}P{^{1}H/^{19}F}) broadband probe), or a Varian Unity Inova 500 MHz NMR equipped with a 5 mm 4-nucleus (^{13}C/^{31}P{^{1}H/^{19}F}) broadband z-axis pulsed field gradient probe. The temperature was calibrated using a methanol or ethylene glycol sample for data collection below or above ambient temperature, respectively. Data were collected first at 20 °C and then in decreasing 10 °C intervals to −40 °C. The samples were then warmed to 20 °C, and spectra were recorded in increasing 10 °C intervals to 100 °C. Upon changing the temperature, samples were allowed 1 min/°C-changed to come to thermal equilibrium. All ^{1}H NMR spectra were referenced to toluene, which appears in trace amounts in all samples (δ = 2.11 ppm).

Table 4. Room-Temperature ^{13}C NMR Chemical Shifts for 1, 2a, 2b, and Representative Zirconocenium Pyridyl Complexes (500 MHz, C_6D_5Cl)

	δ (ppm)	multiplicity	integration	assignment
1	35.0	s	2	$ZrCH_3$
	98.4	s	4	Cp
	124−130	m	26	Ar-C
2a	39.0	s	1	$CH_3B(C_6F_5)_3^-$
	52.1	s	1	$ZrCH_3$
	101.3	bs	4	Cp
	121−151	m	44	Ar-C
2b	30.5	s	1	Ph_3CCH_3
	52.7	s	1	$ZrCH_3$
	56.1	s	1	Ph_3CCH_3
	102.2	s	4	Cp
	124−151	m	50	Ar-C
4a	1.35	s	1	CH_4
	20.9	s	2	CH_3
	39.0	s	1	$CH_3B(C_6F_5)_3^-$
	98.9	s	2	Cp
	100.2	s	2	Cp
	121−156	m	48	Ar-C
6a	1.35	s	1	CH_4
	23.4	s	2	iPr CH_3
	33.9	s	1	iPr CH
	39.0	s	1	$CH_3B(C_6F_5)_3^-$
	100.0	s	2	Cp
	100.6	m	2	Cp
	120−166		50	Ar-C
7a	1.35	s	1	CH_4
	29.5	s	1	tBu C
	30.3	s	3	tBu CH_3
	39.0	s	1	$CH_3B(C_6F_5)_3^-$
	100.2	s	2	Cp
	100.4	s	2	Cp
	115−170	m	51	Ar-C

NOESY Experiments. Samples were prepared as above and allowed to equilibrate at the experimental temperature for 30 min prior to acquisition unless otherwise noted. Two-dimensional NOESY NMR experiments were performed on the 500 MHz NMR spectrometer using a slightly modified standard three-pulse sequence; specifically, a pulse was added before the relaxation delay to eliminate residual *x*/*y* magnetization. Either 8 or 16 scans of 4096 complex data points (2 × np) in the t_2 dimension were acquired with between 200 and 256 complex data points in F1. The data were multiplied by cosine-squared weighting functions and zero-filled to a 4096 by 4096 matrix (fn and fn1). The 90° ^{1}H pulse widths varied with the experimental conditions (sample and temperature) from 15 to 28 μs. A spectral width of 8000 Hz, a mixing time of 0.3 ms, an acquisition time of 128 ms, and a relaxation delay time of 4 s were used. The number of transients and data points were chosen on the basis of the sample concentration. Baseline correction was used. All NOESY spectra were referenced to toluene, which appears in trace amounts in all samples (δ = 2.11 ppm).

Acknowledgment. This work was supported by the National Science Foundation (CHE-0305436). Financial support from an Evelyn Laing McBain Fellowship to A.L.L. and a William R. and Sarah Hart Kimball Stanford Graduate Fellowship to G.M.W. are gratefully acknowledged.

Supporting Information Available: Pertinent room-temperature and low-temperature 1-D ^{1}H and ^{13}C NMR spectra and 2-D ^{1}H−^{1}H NOESY spectra of the methyl cations and pyridyl complexes are available free of charge via the Internet at http://pubs.acs.org.

OM050473K